ACS OMEGA

http://pubs.acs.org/journal/acsodf

Review

Prospects of Biosensors Based on Functionalized and Nanostructured Solitary Materials: Detection of Viral Infections and Other Risks

Sanjeev Kumar, Ritika Sharma, Bhawna, Akanksha Gupta,* Prashant Singh, Susheel Kalia, Pankaj Thakur, and Vinod Kumar*

Cite This: *ACS Omega* 2022, 7, 22073−22088

Read Online

ACCESS | Metrics & More | Article Recommendations | Supporting Information

ABSTRACT: Advances in nanotechnology over the past decade have emerged as a substitute for conventional therapies and have facilitated the development of economically viable biosensors. Next-generation biosensors can play a significant role in curbing the spread of various viruses, including HCoV-2, and controlling morbidity and mortality. Pertaining to the impact of the current pandemic, there is a need for point-of-care biosensor-based testing as a detection method to accelerate the detection process. Integrating biosensors with nanostructures could be a substitute for ultrasensitive label-free biosensors to amplify sensing and miniaturization. Notably, next-generation biosensors could expedite the detection process. An elaborate description of various types of functionalized nanomaterials and their synthetic aspects is presented. The utility of the functionalized nanostructured materials for fabricating nanobiosensors to detect several types of viral infections is described in this review. This review also discusses the choice of appropriate nanomaterials, as well as challenges and opportunities in the field of nanobiosensors.

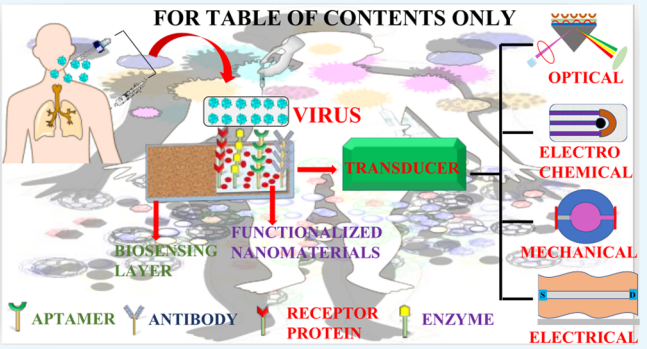

1. INTRODUCTION

Viruses have been posing a constant threat to humanity over the last several decades. Thousands of people have died as a result of various types of microbial infections over the years. Methodologies for early detection and diagnosis were critical in halting the spread of these rapidly transmitted diseases and controlling morbidity and mortality in these conditions. Conventional methods to detect the virus are real-time polymerase chain reaction (qPCR) tests and serological assays. The conventional methodologies for viral infection diagnosis are colossal and, thus, need adroit staff. The conventional methods reported so far are time-consuming, expensive, and labor-intensive.[1] These limitations can be overcome by using nanotechnology in the diagnosis of viral infections. Recently, nanotechnological advances have emerged as a substitute for conventional therapies.

Previous decades have noticed a high surge in biosensor development for detecting several kinds of disorders,[2] fatal diseases,[3] medical conditions,[4] and infectious diseases[5] because they are found to be rapid, simple, sensitive, and accurate. They established their importance by detecting cancer in early stages, checking diabetes, confirming pregnancy, detecting highly transmissible virulent viruses, and many more.[6,7] Biosensor-based devices are composed of bioentities, and the detection mechanism for the bioentities has been represented schematically (Figure 1).[8] The desired features of biosensors are stability, affordability, sensitivity, and accuracy.[9,10] Biosensors detect analytes in the form of electrical, thermal, or optical signals mediated by enzymes or antibodies (Abs).[11,12] These devices have a plethora of applications ranging from clinical to environmental.

Reducing the dimensions to the nano range, i.e., 1−100 nm, could extend the utility of nanomaterials (NMs) because they offer miniaturization and better surface area, which has grabbed immense attention. Due to their nanosize, the ratio of surface to volume increases, and it offers efficient interactions between sensor and analyte. By designing effective interactions between analyte and biosensor, NM-based biosensors have been widely used for the detection of biomolecules and disease diagnostics. A brief discussion of different applications is given in the Supporting Information (SI.1).

Received: February 21, 2022
Accepted: May 16, 2022
Published: June 22, 2022

https://doi.org/10.1021/acsomega.2c01033
ACS Omega 2022, 7, 22073−22088

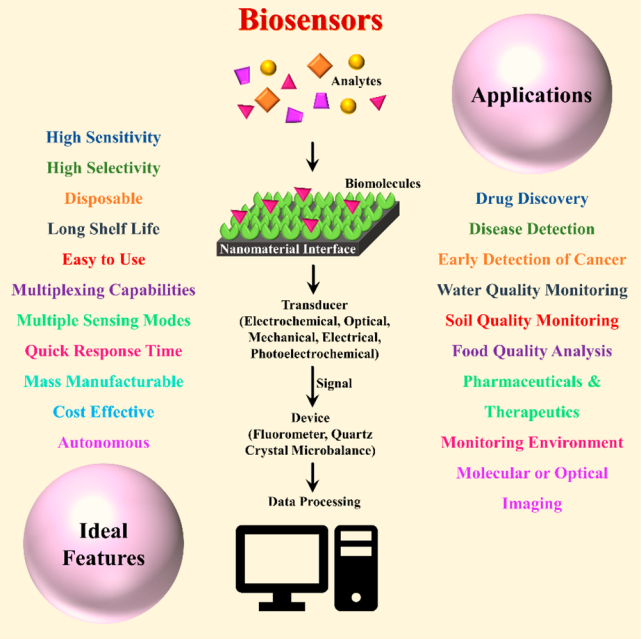

Figure 1. Overview of biosensors representing their ideal characteristics and applications.

The present review summarizes different NM-based biosensors such as metal oxide, single-walled carbon nanotubes (SWCNTs), multi-walled carbon nanotubes (MWCNTs), Au nanoparticles (NPs), and SiO_2-based biosensors and their probable utilization in biomedical applications such as drug delivery, RNA detection, DNA detection, nCoV-2 detection, etc. In addition, the challenges and opportunities available with the nanosensors are also discussed to give insight into the study.

2. DIFFERENT TYPES OF BIOSENSORS FOR DETECTION

Biosensors have multiple advantages when used with nanotechnology, such as real-time analysis, detection using a smaller amount of sample, high-throughput screening, label-free detection, and low limit of detection (LOD).[13−15] Different types of biosensors are known, and a few of them are mentioned in Table 1.

2.1. Optical Biosensors. Optical biosensors provide the opportunity to change the optical properties of the outer surface of the sensor after binding with the analyte, which is then transduced to the detector for sensing (Figure 2A). In the early 1990s, the first surface plasmon resonance (SPR)-based commercial optical biosensor was used. Further, SPR was integrated with optical waveguide grating and biolayer interferometry, making it more effective. They all followed the same principle as affixing targets on the biosensor's surface.[16] The modified biosensor surface was challenged with solutions containing molecules to observe the consequences of binding. The types of optical biosensors, such as colorimetric detection and plasmonic biosensors, are described in the Supporting Information (SI.2). A few examples are label-free miRNA detection,[17] detection of foodborne bacteria,[18] etc.

2.2. Electrical Biosensor. The working of an electrical biosensor is based on the generation of current or voltage on the electrode due to the interaction of the biological sample with an Ab, affirmer, or aptamer. The current and potential values of semiconductors, which were generated by the interaction process at the gate electrode or already have a current-carrying element, were measured with the help of an field-effect transistor (FET) biosensor (Figure 2B). Eveness et al. developed an electric biosensor based on a polyethylene terephthalate-ZnO co-planar electrode to quantify variable amounts of C-reactive protein (CRP). The biosensor included a PET insulating layer between the electrodes and the active ZnO sensor surface.[19] In phosphate-buffered saline (PBS) solution, an In_2O_3 electrically modulated FET biosensing device with great durability was developed and can be employed as a biosensor to respond to miR-21.[20]

2.3. Mechanical Biosensor. Mechanical biosensors have various advantages in detection, such as having a high sensitivity value and being able to instantly process samples without the use of any reagents.[21] A quartz crystal microbalance (QCM) biosensor is a piezoelectric-type sensor that detects the whole bacterial cell by altering resonance frequency. When modified with NPs, it generates an amplified signal to be used in detection (Figure 3A). Zhang et al. fabricated an integrated optomechanical cantilever sensor that contained a rib waveguide. The rib waveguide cantilever was connected with hidden waveguides on silicon.[22] For human serum albumin detection, a surface stress mechanical biosensor based on a double-sided Au NP-coated grid-type polydimethylsiloxane membrane and 3D printing has been developed.[23]

2.4. Electrochemical Biosensor. An electrochemical biosensor is used to transduce the sensing target molecule into digital electrochemical signals (Figure 3B).[24,25] When combined with NMs, the electrochemically active surface area of the biosensor increases, and also, the electron-transfer efficiency was accelerated.[25,26] The key advantages were high sensitivity, simplicity, low cost, label-free sensors, and ease of miniaturization, and none of these were affected by the analyte present in the matrix. However, certain drawbacks remain, such as high LOD, inconsistent reproductivity, and no specific binding.[27,28] Recently, prussian blue/reduced graphene oxide (RGO) films co-assembled through electrostatic interaction have been successfully synthesized for wearable biosensors and were reported to be used for the detection of glucose.[29] Moreover, a multi-channel sweat biosensor technology for quantitative analysis of sweat that was based on a fully integrated patch-type array was reported.[30]

2.5. Photoelectrochemical Biosensor. A photoelectrochemical (PEC) biosensor is a new analytical approach that is associated with the charge-transfer process between a photoactive material, an electrode, and an analyte under light illumination. The completely separated and different energy forms of light and detection signals result in potentially high sensitivity and lower background signals to analyze the target.[31] It consists of three essential components: (a) a photocatalyst semiconductor immobilized on a transparent substrate having high conductivity as the working electrode, (b) an electrocatalyst counter electrode, and (c) an appropriate electrolyte. The photocatalyst semiconductor absorbs light radiation and generates charge carriers at the working electrode (photoanode). The charge collector receives electrons injected from the photocatalyst's conduction band (CB), while biological organisms present in the electrolyte scavenge holes in the valence band (VB) of the photocatalyst.[32] Zhao et al. constructed a PEC biosensor based on a Co_3O_4−Au polyhedron to detect miR-141. Through the particular interaction of streptavidin−biotin, biotin-modified DNA was

https://doi.org/10.1021/acsomega.2c01033
ACS Omega 2022, 7, 22073−22088

Table 1. Comparative Analysis of Various Types of Biosensors

biosensors	optical	electrical	mechanical	electrochemical	photoelectrochemical
principle	optical property changes on sensor's surface after analyte binding	current or voltage changes on electrode after analyte binding	oscillation at specific resonant frequency that changes by increasing mass on surface	transduce target molecule into digital electrochemical signals	charge-transfer process between photoactive material, an electrode, and an analyte under light illumination
analytes	enzymes, antibodies, nucleic acids, aptamers	antibody, affirmer, or aptamer	microbial cell, antibody, nucleic acids	enzymes, antibodies, DNA, aptamers	enzymes, antibodies, DNA, aptamers
change detected	optical properties, fluorescence, and absorbance	current or voltage changes on the electrode	resonant frequency of crystal due to change in mass	redox reaction/electrical conductivity as a result of change in ion concentration	charge transfer under light illumination
technique used	SPR or LSPR	potentiometric	QCM	amperometric	
	colorimetric	conductometric	cantilever technology	impedimetric	
		FET			
		voltammetric			
		impedance			
advantages	simple	multiplex label-free detection	high sensitivity	high selectivity and sensitivity over optical biosensors	high sensitivity and lower background signals to analyze the target
	cost-effective	high specificity and sensitivity	instant response time	lower purchase cost	
	rapid detection method without analytical equipment		simple miniaturization process	rapid results	
			high throughput	better signal-to-noise ratio	
limitations	low sensitivity	translation to clinical samples	requires temperature control	low LOD over other biosensors	
	limited capability of a multiplex	buffered solution may interfere	sensitive to sample matrix effect	inconsistent reproductivity	
				no specific binding	
sensitivity and precision	depends on NMs binding with biosensor	depends on NMs binding with biosensor	depends on NMs binding with biosensor	depends on NMs binding with biosensor	depends on NMs binding with biosensor

https://doi.org/10.1021/acsomega.2c01033
ACS Omega 2022, 7, 22073−22088

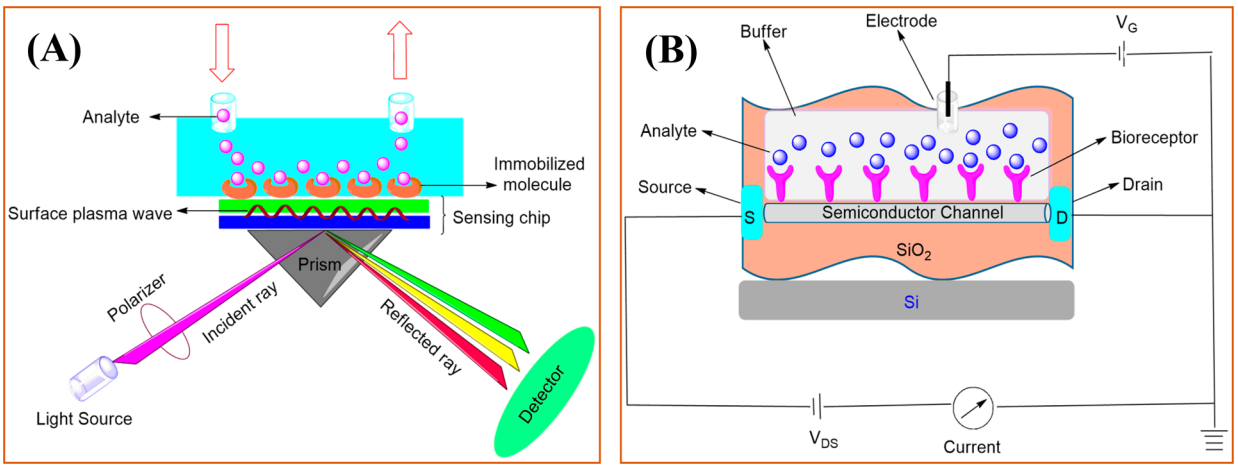

Figure 2. Schematic of (A) optical biosensor and (B) FET biosensor for detection.

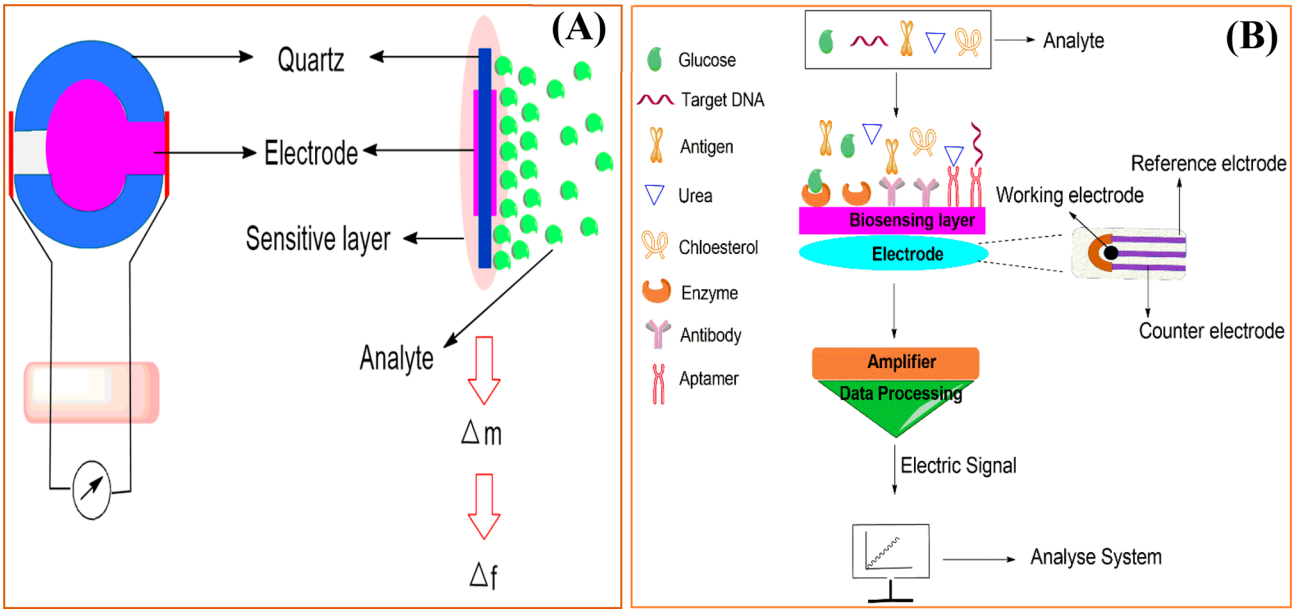

Figure 3. Schematic of (A) QCM and (B) electrochemical biosensor.

deposited on ITO/TiO_2/Bi_2S_3 to link streptomycin-modified Co_3O_4–Au.[33] Moreover, it was constructed based on a TiO_2/2D coordination polymer $CuCl_x$(4-mercaptobenzoic acid)$_y$ photoelectrode by Yang et al. for the detection of miR-21.[34]

3. FUNCTIONALIZED NANOMATERIAL-BASED BIOSENSORS

Nanotechnology and nanoscience deal with the properties of materials utilized for various applications via miniaturization. Integrating nanotechnology with medical science opens a new dimension for new therapeutic approaches at the nanoscale. NPs can be used as a vehicle to carry the drug-like molecule to the target site. These possess a variety of compositions and structures that allow them to possess unique physicochemical properties and open new horizons for various biomedical applications.[35] The properties of functionalized NMs as biosensors can be enhanced by surface modification.[36] They are next-generation smart materials with myriad applications. The following section explores several functionalized NM-based biosensors for biosensing capabilities.

3.1. Metal Oxide-Based Biosensors. Metal oxides are versatile materials possessing features like high surface-to-volume ratio, light excitation, and wide bandgap semiconductors[37,38] and can be easily integrated into the development of biosensors. In the past few years, biosensors based on metal oxides were developed for various purposes such as detection of H_2O_2, urea, and glucose[39] and even for cancer cell and virus detection.[40,41]

In the case of enzyme-immobilized biosensors, an enzyme was immobilized on the surface of nanostructured metal oxide (NMO)-based electrodes without affecting the configuration of the enzyme–matrix binding conformation. This leads to increased signal transduction and stability of biosensors.[42,43] In the case of glucose-based biosensors, glucose oxidase (GO_x) was immobilized on NMOs.[44,45] In another case, GO_x was immobilized by the chemical etching of ZnO nanorods through the cross-linking process and electrochemically impregnated with Au NPs.[46] GO_x and horseradish peroxidase (HRP) immobilized on a carbon-based ZnO (C-ZnO) nanowire array have been reported to perform at low LOD with high sensitivity.[47] Glucose biosensors based on CeO_2

https://doi.org/10.1021/acsomega.2c01033
ACS Omega 2022, 7, 22073−22088

Table 2. Functionalized SWCNT Biosensor for the Detection and/or Conjugation with Biomolecules

s. no.	materials used for surface modification	synthesis method	application	ref
1	PEG	RF-CCVD method	drug delivery	56
2	PEG		cancer drug delivery and imaging tool	57
3	human serum protein		biological application and binds with siRNA	60
4	CTAB		binding with siRNA oligonucleotides	58
5	HMDA and PDDA		delivery of siRNA	59
6	PL−PEG		delivery of siRNA and gene silencing	61
7	$-NH_3^+$		gene delivery and delivery of plasmid DNA	62
8	$-Lys\text{-}NH_3^+$		gene delivery and delivery of plasmid DNA	62
9	biotin		tumor-targeted drug delivery	63
10	DNA	reflux process followed by addition of DNA	determination of daunorubicin anti-cancer drug	64
11	mesoporous silicon	facile stain-etching and sonothermal process	detection of non-enzymatic glucose	65

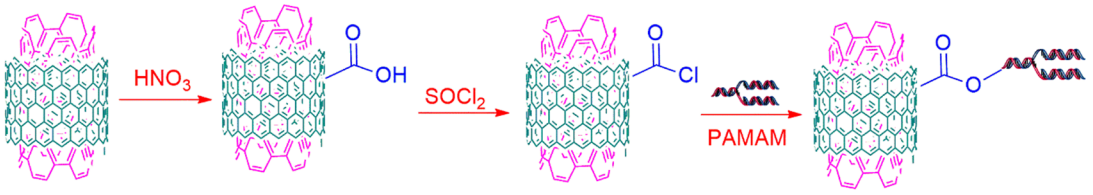

Figure 4. Schematic of the synthesis of PAMAM-MWCNTs.

films on platinum-coated glass plates using pulsed laser deposition were also used.[48] Immobilized GO_x on Fe_3O_4 by a physical adsorption process was developed to detect mediator-free glucose, and it showed high sensitivity.[49] Another glucose biosensor was based on the electrochemical deposition of GO_x and NiO_x NPs on a glassy carbon electrode (GCE), providing real-time glucose monitoring.[50] The nanocomposite of ZnO NPs on a GCE was developed with high sensitivity.[51]

In the case of an optical immunosensor, the efficiency is dependent on the silanized TiO_2. Fabrication of an anti-α-fetoprotein (AFP) sensor was developed using immobilized AFP on a nanocomposite of TiO_2 and CH, providing a low detection limit of 0.1 ng mL^{-1}. On the other hand, an AFP sensor based on immobilizing anti-AFP onto a Au NP surface electrodeposited on a CH-MnO_2/MWCNT-Ag nanocomposite on GCE exhibited a 0.08 ng mL^{-1} LOD.[52,53] CeO_2 film and ZnO NP on indium tin oxide (ITO) glass were used to co-immobilize rabbit IgG and bovine serum albumin (BSA) for ochratoxin A (OTA) detection using electrochemical impedance spectroscopy (EIS). This provides improved sensitivity and rapid response time.[43] Currently, NMO-based biosensors have attracted much attention as immobilizing matrixes to develop various biosensors. NMO such as Zn, Fe, Mg, etc. possess various properties such as non-toxic, biocompatibility, etc. A recent study showed that biosensors' improved characteristics could be achieved by incorporating NPs with NMOs.[54] The exceptional properties of NMOs could offer many prospects for the fabrication of biosensing devices to address future needs for diagnostic tools. The unique properties are due to the high surface-to-volume ratio, the ability of adsorption, etc. It is important to select a suitable NMO for fabrication of an efficient biosensor because the binding between NMO and the biomolecule determines the performance of the biosensor. This binding is crucial for establishing a biocompatible environment as the biomolecule activity is highly stable. This provides opportunities for biosensor development with low cost, high sensitivity, long shelf life, and low LOD.[55]

3.2. SWCNT-Based Biosensors. Zhang et al. demonstrated functionalization with polyethylene glycol (PEG). First, SWCNTs were coated with a −COOH functional group followed by $SOCl_2$ that generated a −COCl group on the surface of the SWCNTs. Further, it was mixed with PEG to form PEG-SWCNTs and thereby reduced cytotoxicity, caused less membrane damage, and increased biocompatibility. The SWCNTs had a unique surface chemistry and fibrous structure that helped in the growth of SWCNTs in the cell membrane and then transferred them to the cytoplasm. The nanotubes interacted with the mitochondria in the PC12 neuronal cell and controlled the gene present in the metabolic process, and they showed good drug delivery results.[56] Bhirde et al. also reported modification with PEG used to deliver cisplatin anticancer drugs in the infected mice. For the modification, carboxylated SWCNTs were reacted with amine-terminated PEG with the help of 1-ethyl-3-(3-dimethylaminopropyl)-carbodiimide hydrochloride (EDC)/*N*-hydroxysuccinimide (NHS) as an amidization promoter, as shown in Figure SI.3.[57] Yan et al. modified it with cetyltrimethylammonium bromide (CTAB) via a sonication process (Figure SI.4) that caused binding with small interfering RNA (siRNA).[58] Krajcik et al. proposed functionalization with poly-(diallyldimethylammonium chloride) (PDDA) and hexamethylenediamine (HMDA) (Figure SI.5). The desired nanotube was oxidized via a reflux process followed by the treatment of carboxylic acid-activated SWCNTs with HMDA, $SOCl_2$, and NEt_3 in a dimethylformamide (DMF) solution. HMDA has protonated amines ($-NH_4^+Cl^-$) that generates a positive charge on the nanotube, while PDDA generates a more positive charge on SWCNTs than HMDA. siRNA was bound with PDDA-HMDA-SWCNTs (**1**), which helped as a carrier to enter siRNA in the cell, and siRNA was liberated into the cytosol, enhancing gene silencing. Also, **1** decreased the cytotoxic side effect as compared to other liposomal transfection solutions.[59] See Table 2 for details. More SWCNT-based biosensors are provided in the Supporting Information (SI.3).

https://doi.org/10.1021/acsomega.2c01033
ACS Omega 2022, 7, 22073−22088

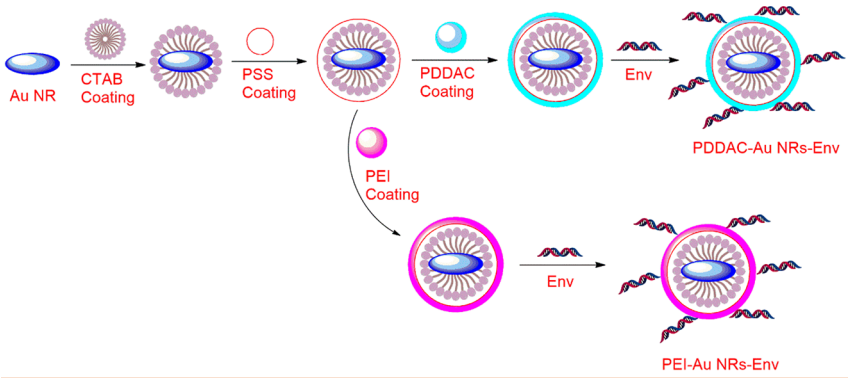

Figure 5. Schematic of Au NRs to form a Au-Env complex.

Table 3. Activation of a Au Molecule for Sensing and/or Conjugation with Biomolecules

s. no.	materials used	synthesis method	application	ref
1	PDDA	electrostatic layered assembly	DNA vaccine delivery for HIV treatment	68
2	PEI	electrostatic layer assembly	DNA vaccine delivery for HIV treatment	68
3	pRNA		biosensor for sensing of miRNA	69
4	aptamer		biosensor for sensing of adenosine	71
5	DNA		optimized biosensor for detection of miRNA	70
6	silsesquioxane	layer-by-layer deposition method	label-free DNA biosensor for Zika virus detection	72
7	DNA		amplified electrogenerated chemiluminescence, biosensing for the detection of thymine DNA glycosylase	73
8	PEG	chemical reduction method	biosensor for the detection of ssDNA	74
9	citrate	citrate reduction method	sensing of hepatitis C RNA virus by colorimetric gene sensor	75
10	core−shell Fe_3O_4−Au NPs/PNA		biosensor for detection of miRNA	76

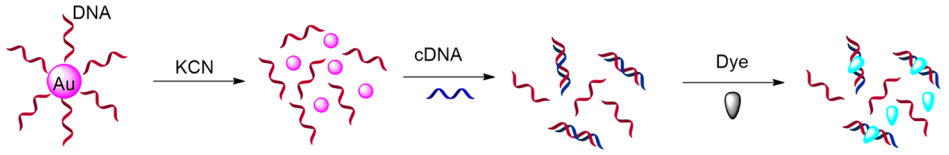

Figure 6. Principle of assay for the staining of dsDNA dye for quantification.

3.3. MWCNT-Based Biosensors. Singh et al. reported ammonium functionalized MWCNTs (f-MWCNTs) (Figure SI.8) for effective performance in gene delivery. f-MWCNTs similarly condensed DNA as f-SWCNTs did. Among these three f-CNTs, MWCNT-NH_3^+ condensed a larger amount of DNA than the other two functionalized CNTs because MWCNTs provide a larger surface area to interact with DNA.[62] Tao et al. reported the metal templating using poly(amidoamine) dendrimer (PAMAM) f-MWCNTs. For synthesis, MWCNTs were reacted with nitric acid to give a carboxyl group at the surface. Further, it reacted with thionyl chloride to form their acid chloride derivative followed by conjugation via ester linkage with hydroxyl-functionalized dendrons to give PAMAM-MWCNTs (Figure 4).[66] Yu et al. published the condensation of DNA and increased gene-transfer process using a polyethyleneimine (PEI)-activated MWCNT heterostructure. The heterostructure was formed when MWCNTs reacted with acid to coordinate the carboxylic group, followed by PEI with the help of EDC/NHC coupling that covalently bound MWCNTs.[67]

3.4. Au NP Based Biosensors. Yu et al. reported Env plasmid DNA vaccine delivery for HIV treatment in infected mice using poly(diallydimethylammonium chloride) (PDDA) and PEI f-Au nanorings (NRs). To synthesize f-Au NRs, Au NRs were mixed with a precursor to form the seed solution of CTAB-Au NRs. After that, CTAB-Au was coated with poly(styrene sulfonate) (PSS), which led to forming negatively charged Au NRs followed by a reaction with PDDA or PEI to get f-Au NRs. For Au NRs as vaccine adjuvants, NRs were coated with contrasting surfaces, and Env led to the formation of a Au-Env complex (Figure 5).

Here, transmission electron microscopy (TEM) images revealed that the sizes of the Au NRs were similar in all three cases; thus, the physicochemical properties of CTAB, PEI, and PDDA affected the overall biosensor performance (Figure SI.9). The author examined the improvement of Env DNA's immunogenicity with these two f-NRs and found that f-NRs with Env gave less immune response, even lower than that of naked Env DNA.[68] Lee et al. proposed mono f-Au NPs with packaging RNA (pRNA) to sense miRNA using the electrochemical surface-enhanced Raman spectroscopy (SERS) technique. In this, one copy of a pRNA three-way junction (RNA 3WJ) with Sephadex G100 aptamer and biotin on each arm was immobilized to Sephadex G100 resin, resulting in conjugation with one Au NP. The formed complex was bound to streptavidin-coated Au NP via streptavidin−biotin inter-

https://doi.org/10.1021/acsomega.2c01033
ACS Omega 2022, 7, 22073−22088

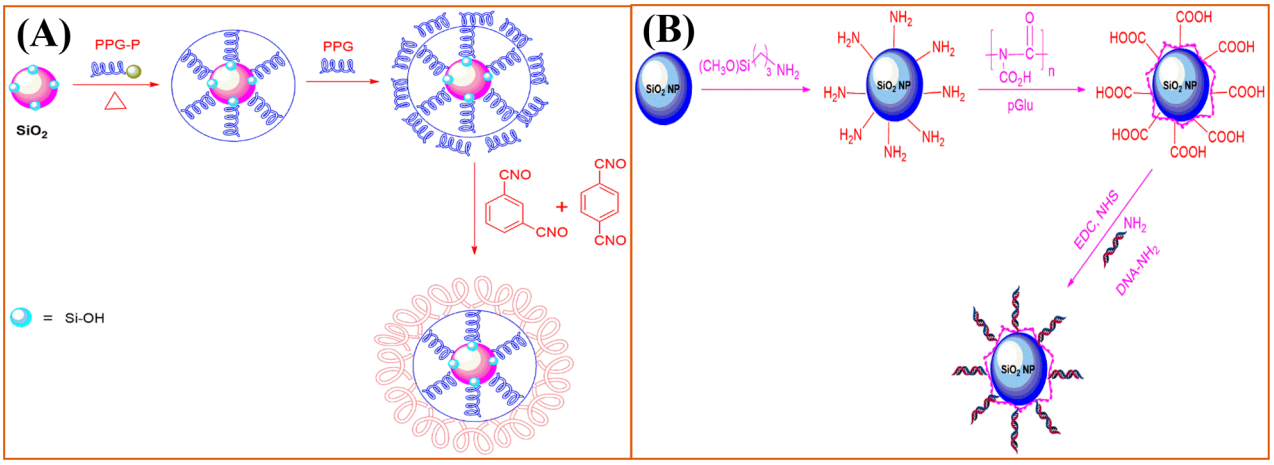

Figure 7. Schematics of (A) dispersion of modified SiO_2 into the PU matrix and (B) synthesis of ssDNA f-SiO_2 NPs.

Table 4. Various Applications of Engineered SiO_2 Particles

s. no.	materials used for surface modification	particle size	synthesis method	application	ref
1	PPG-P	30 nm	in situ polymerization	uniformly distributed the NPs in polyurethane matrix	77
2	APTES	68 nm	water-in-oil microemulsion method	mechanical strength, thermal stability, and gas permeability	78
3	MPTMS	32 nm	water-in-oil microemulsion method	enhancement in mechanical strength, thermal stability, and gas permeability	78
4	PTMS	34 nm	water-in-oil microemulsion method	enhancement in mechanical strength, thermal stability, and gas permeability	78
5	VTES	38 nm	water-in-oil microemulsion method	enhancement in mechanical strength, thermal stability, and gas permeability	78
6	5′-phosphorylated ssDNA	120 ± 5 nm	layer-by-layer electrostatic adsorption	capture and detection of single-stranded RNA	79

action followed by purification and reassembly with one more 3WJ, leading to the formation of 3WJ/Au NP.[69] Hwu et al. demonstrated activation of Au NPs with DNA on a GCE for optimized biosensor-based miRNA detection (Table 3). The conjugated DNA-Au NPs were prepared by mixing reduced DNA and sodium dodecyl sulfate (SDS) with Au NPs and retaining it for incubation. After that, NaCl and PBS were also mixed with the sonicating method. The principle of the assay was to remove DNA attached to the surface of Au NPs by dissolving it in potassium cyanide. Then, these strands were hybridized with their complementary DNA (cDNA), and a fluorescence readout was done by staining double-stranded DNA (dsDNA) with dye (Figure 6).[70] More Au NP-based biosensors are provided in the Supporting Information (SI.4).

3.5. SiO_2 NP-Based Biosensors. The SiO_2 NPs tend to form aggregates due to their high surface energy. This results in improper distribution into the polyurethane (PU) matrix. To overcome this, Gao et al. modified the SiO_2 NPs surface with poly(propylene glycol) phosphate ester (PPG-P) (Figure 7A); PPG-P was prepared via the esterification process of polyphosphoric acid and PPG. The f-SiO_2 NPs showed a decrease in surface energy, increase in stability, no aggregation, and uniformly distributed SiO_2 NPs into the PU matrix.[77]

Naka et al. published the organo f-SiO_2 NPs as 3-aminopropyltriethoxysilane (APTES), 3-mercaptopropyltrimethoxysilane (MPTMS), phenyltrimethoxysilane (PTMS), and vinyltriethoxysilane (VTES), which led to enhanced mechanical strength, thermal stability, and gas permeability of the polymer material. The f-SiO_2 NPs are denoted as SNP, AP-SNP, MP-SNP, P-SNP, and V-SNP, respectively. TEM images of organo f-SiO_2 NPs are shown in Figure SI.12. The D_{max} values measured for the SNP, AP-SNP, MP-SNP, P-SNP, and V-SNP were 33, 63, 63, 50, and 36 nm, respectively. The functionalization of SiO_2 led to enhanced NP dispersion uniformly in the polymer matrix, a strong force of interaction to solid materials, and a selective bond formed with certain functional groups of the polymer chain to increase the polymer's mechanical property and thermal stability.[78] Zhou et al. proposed 5′-phosphorylated single-stranded DNA (ssDNA)-modified SiO_2 NPs with T4 RNA ligase to seize and detect 20−24 base subpicomolar concentrations of ssRNA from target solution and remain stable in the presence of dithiothreitol (DTT). The modified ssDNA-SiO_2 NPs can be denatured and hybridized again and again. ssDNA-SiO_2 NPs were synthesized by a reaction of aminopropyl silane with a silanol group in which attachment of the amino group to the surface of the Si NPs occurred. After that, amino-modified SiO_2 NPs adsorbed the monolayer of poly-L-glutamic acid (pGlu) via electrostatic interaction on its surface. In the next step, the carboxylic functional group of pGlu formed a covalent bond with amino groups on the surface of SiO_2 NPs and 5′-phosphorylated, 3′-amino-activated ssDNA to form an amide with the help of EDC/NHS in a single step (Figure 7B).[79] See Table 4 for details.

3.6. BNNT-Based Biosensors. Lahiri et al. functionalized boron nitride nanotubes (f-BNNTs) with polylactide−polycaprolactone copolymer (PLC), enhancing the biocompatibility and mechanical strength and providing applications in orthopedic scaffolds. The mechanical properties of f-BNNTs were enhanced due to increased tensile strength up to 109%

https://doi.org/10.1021/acsomega.2c01033
ACS Omega 2022, 7, 22073−22088

and elastic modulus up to 1370%. Also, functionalization enhanced the uniform distribution along with excellent interaction with the polymer matrix. The pure BNNT cytotoxicity investigated with macrophage and osteoblast cells resulted in no increase in the number of cell deaths.[80] Ciofani et al. demonstrated the cytocompatibility of human neuroblastoma cells by BNNTs. The authors showed no inauspicious effect of BNNTs on cell replication, viability, and metabolism. The functionalization of BNNTs with PEI enhanced the interaction of the nanotube with the living cells. The material was conjugated with fluorescent probes for incubation with the cells. The internalization of the f-BNNTs by the cells was confirmed by an uptake assay, which illustrated that the mechanism of uptake of the material was dependent on the energy and chemical reactivity of PEI. The enhancement in the chemical reactivity of the nanotube by coating with PEI is what makes the interaction of the material with biological complexes possible.[81] Emanet et al. proposed the modification of BNNTs with glucose, starch, and lactose to study the increment of their diffusibility in an aqueous solution for biocompatibility and cellular uptake. In the synthesis of modified BNNTs, the nanotube that was reacted with hydrogen peroxide resulted in the attachment of −OH groups on the outer part of the nanotubes. Further, carbohydrates and −OH groups were attached to hydroxylated BNNTs by using glutaraldehyde as a cross-linker (Figure 8). Among all of the

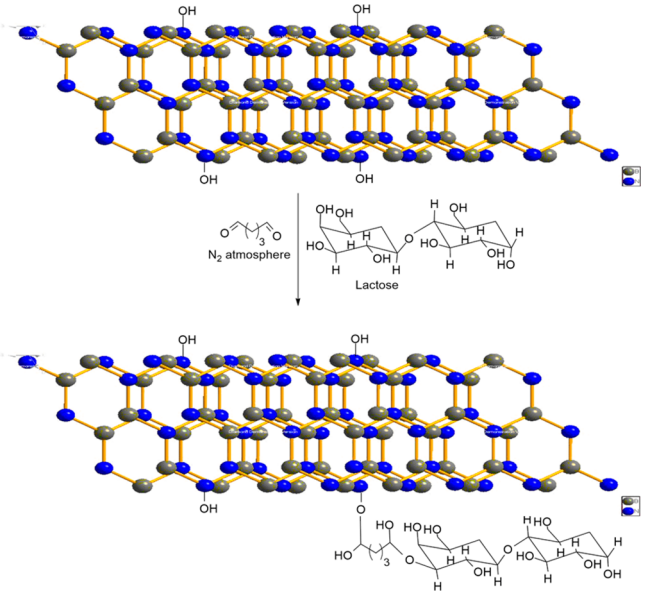

Figure 8. Schematic of a modification of BNNTs with carbohydrate.

carbohydrates, glucose was very small and bound strongly with the −OH group of hydroxylated BNNTs. Unmodified BNNTs had a hydrophobic nature, which caused toxicity at high doses on adenocarcinoma human alveolar basal epithelial cells (A549) and human dermal fibroblasts cells. This toxicity of unmodified BNNTs was reduced to a specific value by modifying it with carbohydrates even at a high number of doses.[82] See Table 5 for details.

3.7. Upconverting Nanoparticle-Based Biosensors. Jiang et al. demonstrated the modification of silica-coated upconverting nanoparticles (UCNPs) with the amino group and their application in siRNA delivery to the target cell and fluorescence imaging. Modified UCNPs were conjugated with

Table 5. Modified BNNTs Used in Various Applications

s. no.	materials used	application	ref
1	PLC	biocompatibility, mechanical properties	80
2	PEI	biomedical applications	81
3	glucose	biomedical applications and interaction with protein	82
4	lactose	biomedical applications and interaction with protein	82
5	starch	biomedical applications and interaction with protein	82
6	glycol−chitosan	biomedical applications	83

the Her2 Ab with covalent bond formation between carboxylic acid moieties and amino moieties of Ab. They modified NPs to fluorescence labeling of Her2 receptors on SK-BR-3 cells and siRNA delivered to SK-BR-3 cells. Also, the modified NPs conjugated with folic acid on their surface were used to label the folate receptors fluorescently on HT-29 cells.[84] Mi et al. demonstrated the formation of a nanocomposite via conjugation of carboxylic group-functionalized Fe_3O_4 and amine-functionalized UCNPs coated with silica, with applications in biomedicine. For the synthesis of the nanocomposites, Fe_3O_4 was functionalized with the carboxylic group on its surface via the coprecipitation method, and silica-coated UCNPs were functionalized with an amine group on their surface via the Stober process. Further, these two NPs conjugated with each other with the help of EDC and NHS by the formation of a covalent bond and formed an Fe_3O_4/UCNP nanocomposite (Figure 9). The nanocomposites had a chemically active amine

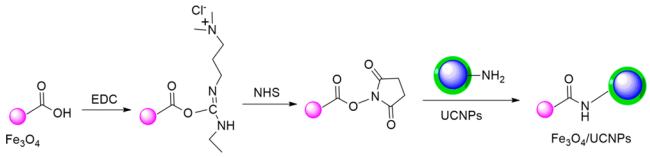

Figure 9. Schematic of the synthesis of Fe_3O_4/UCNP nanocomposite.

group on UCNPs and carboxylic groups on Fe_3O_4, which conjugated with a protein such as transferrin. It was used to acknowledge that transferrin receptors were overexpressed on HeLa cells and for biolabeling and fluorescent imaging of HeLa cells (Figure SI.13).[85]

Yuan et al. synthesized the UCNP@SiO_2@Ag nanocomposite and modified it with DNA to enhance its biocompatibility and reduce the cytotoxicity; it was used in cell imaging applications. First, the UCNPs were coated with the silica shell on their surface via a reverse microemulsion process. Further, Ag NPs were grown on Si-coated UCNPs. For Ag NPs, Si-coated UCNPs were reacted with (3-mercaptopropyl)triethoxysilane (MPS) to form a thiol bond on the surface, followed by reduction of $AgNO_3$ to introduce the Ag NPs (Figure 10). The silica prevented contact of the Ag NPs to the UCNPs as a spacer molecule in the nanocomposites. DNA was used for the modification of the nanocomposite to enhance the biocompatibility. To reduce the cytotoxicity of Ag NPs, DNA was used as a capping agent that covered the positively charged Ag NP surface with its negatively charged surface.[86] See Table 6 for more details. More UCNP-based biosensors are provided in the Supporting Information (SI.5).

https://doi.org/10.1021/acsomega.2c01033
ACS Omega 2022, 7, 22073−22088

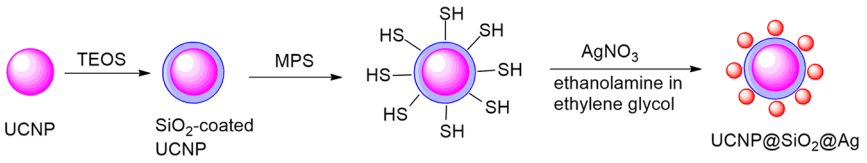

Figure 10. Schematic of the synthesis of UCNP@SiO_2@Ag nanocomposite.

Table 6. Activated UCNPs with Application in Sensing and/or Conjugation with Biomolecules

s. no.	surface modification	materials used	synthesis method	particle size	application	ref
1	$NaYF_4$:Yb,Er	streptavidin			DNA sensor	87
2	$NaYF_4$:Yb,Er@SiO_2	amino group		30 nm	delivery of siRNA	84
3	$NaYF_4$:Yb,Tm@ SiO_2	PEG spacer carrying NHS groups	reverse microemulsion method	38 nm	protein conjugation	88
4	$NaYF_4$:Yb,Er@SiO_2	amino-ethoxy silane		50 nm	bioimaging and conjugate with biomolecules	89
5	$NaYF_4$:Yb,Er@SiO_2	antibody	glutaraldehyde spacer method		bioimaging and conjugate with biomolecules	89
6	$NaYF_4$:Yb,Er@SiO_2	anti-Cx43	glutaraldehyde spacer method		bioimaging and conjugate with biomolecules	89
7	$NaYF_4$:Yb,Er	Fe_3O_4		100−150 nm	biolabeling, imaging of cancer cells, and conjugation with biomolecules	85
8	$NaYF_4$:Yb,Er@ SiO_2@Ag	DNA	reverse microemulsion process		conjugate with DNA and cell imaging	86

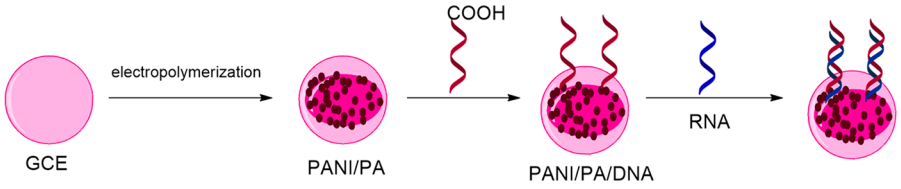

Figure 11. Schematic of the synthesis of biosensors based on PANI/PA polymer hydrogel.

3.8. Other Materials-Based Biosensors. Yang et al. synthesized phytic acid (PA)-functionalized polyaniline (PANI/PA) polymer hydrogel via an electrochemical copolymerization process for the electrochemical detection of miRNA (Figure 11).

In the synthesis of a functionalized polymer, 3-aminophenylboronic acid (ABA) and aniline were reacted and a boronic acid species was inserted into PANI chains. Boronic acid acted as a cross-linker between PANI and PA in the preparation of PANI/PA. The polymer was deposited on the GCE surface. For electrochemical biosensors, DNA was covalently attached through a $-NH_2$ group on the surface of the polymer. PA had high biocompatibility and hydrophilicity, while PANI had higher electrochemical properties; these properties of both PA and PANI make a copolymer that is a good electrochemical biosensor.[90] Fan et al. proposed the functionalization of CdS NRs with beta-cyclodextrin (β-CD) (f-CdS NRs) for electrochemical HIV DNA detection by connecting with a catalytic hairpin assembly mediated with DNAzyme catalyst, forming an insoluble precipitate. CdS NRs were synthesized via the hydrothermal method by adding $Cd(NO_3)_2{\cdot}4H_2O$ and $SC(NH_2)_2$ in ethylenediamine in the Teflon autoclave reactor, leading to the formation of a yellow suspension. For f-CdS NRs, synthesized CdS NRs with carboxymethyl-β-cyclodextrin were uniformly dispersed in PBS (5.3 pH) with EDC/NHS (Figure 12).[91]

Wang and Hui synthesized PEG-activated polypyrrole nanowires (Ppy NWs) via electrochemical oxidation of NH_2 present on PEG, which covalently attached with Ppy NWs. PEG-Ppy NWs were immobilized on GCE followed by binding

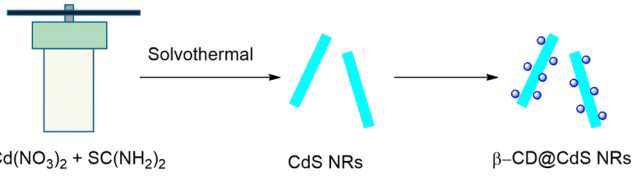

Figure 12. Schematic of the synthesis of β-CD-functionalized CdS NRs.

with a DNA probe. Methylene blue was used as a redox indicator to detect signals through the differential pulse voltammetry method. PEG-Ppy NWs were used for a biosensor to detect miRNA (Figure 13).[92]

Ppy NWs were immobilized on GCE via electrochemical polymerization containing PBS, Py, and *p*-toluene sulfonate acid at a 0.75 V constant potential value. Further, PEG-NH_2 was mixed with $LiClO_4$ to attach through covalent bonding on the Ppy NWs surface. Lastly, the product was mixed with 1.0 μM carboxyl-functionalized ssDNA and EDC/NHS solution to covalently immobilize ssDNA on the PEG-NH_2.[92] Scanning electron microscopy (SEM) images of f-Ppy revealed that the Ppy NWs were arranged in a vertical position on the surface of the electrode to form one-dimensional NWs (Figure SI.17).[92] See Table 7 for more details. Other materials-based biosensors are provided in the Supporting Information (SI.6).

3.9. Utilization of Biosensors in Detection of COVID-19. Conventional methods for the detection of COVID-19 were based on reverse transcriptase quantitative polymerase chain reaction test (RT-qPCR), chest X-ray, computed tomography (CT) scan, and serological assessment of elevated

https://doi.org/10.1021/acsomega.2c01033
ACS Omega 2022, 7, 22073−22088

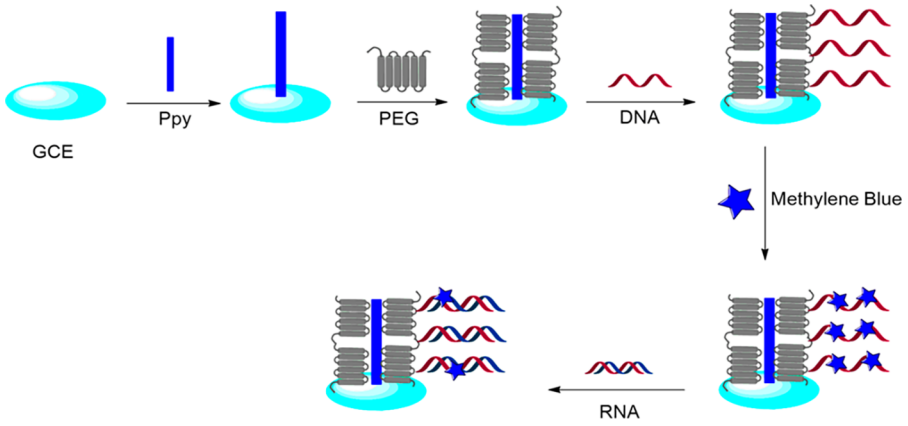

Figure 13. Schematic of the detection of microRNA using PEG-activated Ppy NWs.

Table 7. Modification of Various Particles Used for Sensing and/or Conjugation with Biomolecules

s. no	surface modification	materials used	particle size	synthesis method	application	ref
1	PANI	PA		electrochemical copolymerization	electrochemical detection of miRNA	90
2	CuO NPs	dopamine	30 nm	microwave-assisted methodology	colorimetric biosensor for detection of cysteine	93
3	Gd_2O_3 NRs	aspartic acid	14.26 ± 0.13 nm		electrochemical biosensor for detection of vitamin D_3	94
4	CdS NRs	β-CD	25−40 nm	solvothermal method	PEC biosensor for detection of HIV DNA	91
5	PtCo mesoporous nanosphere	DNA	43.82 nm		electrochemical immunodetection of N^6-methyladenosine RNA	95
6	Ppy NW	PEG	300 nm	electrochemical oxidation	biosensor for detection of miRNA	92
7	CuO NPs	streptavidin			lateral flow strip biosensor for the sensing of human papillomavirus (HPV) type 16 DNA	96
8	dopamine	aggregate induced emission dye (TPE-BTD)			for detecting H_2O_2, G-quadruplex DNA, glucose, and Dam MTase solid	97
9	CRISPR/Cas 13a system	catalytic hairpin DNA circuit			detection of multiple RNA	98
10	CRISPR/Cas 13a	$Ti_3C_2T_x$/PEDOT:PSS			detection of nucleic acid using wireless sensor	99

levels of CRP, interleukin 6 and 10, etc. (Figure 14).[100,101] However, in some cases, these methods do not give accurate results, which is a serious limitation in exploring these methods or protocols. To overcome this issue, there was a dire need for point-of-care biosensors as a detection strategy to control morbidity and mortality when no drug or vaccine specific for the virus was available.[102,103] Other methods to detect COVID-19 are described in the Supporting Information (SI.7). Biomarkers in blood can be used as a prognostic for disease detection. Recently, smell dysfunction as a biomarker was proposed for COVID-19; therefore, biosensors for mucus protein detection can be helpful for early diagnosis.[104] It should be noted that other diseases also had reported nasal dysfunction, and therefore, it may not be specific for COVID-19.[105] In previous years, some biosensors had been developed for ROS detection, leading to another route for COVID-19 detection.[106]

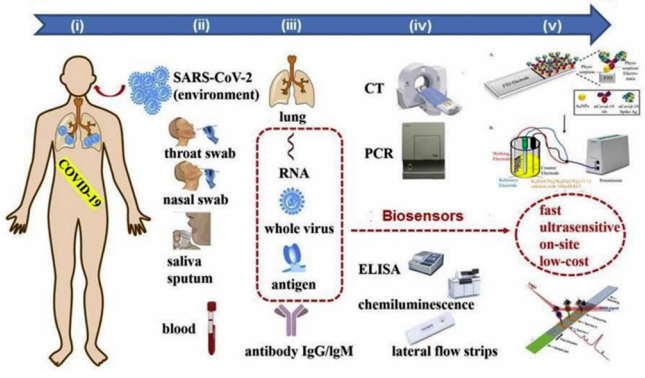

Figure 14. Schematic of currently used diagnostic techniques and possible biosensing platforms for COVID-19. Reprinted with permission from ref 107. Copyright 2020 Elsevier B.V.

4. DEVELOPMENT OF BIOSENSORS

An important plan of action could be the invention of NM-based biosensors to recognize and neutralize an epidemic caused by microbes. It would open new prospects to stop an outbreak of various viruses by identifying molecular species in real time. Patra and co-workers are working on sensor development based on semiconductors or hybrid NMs that show rapid viral identification of ultralow concentrations.[108−110] Hwang et al. fabricated FETs with a graphene channel (gFETs) to recognize DNA/RNA with accuracy and high sensitivity.[111] The NMs of quantum dot (QD)-RNA oligonucleotide can diagnose hepatitis C virus NS3 protein selectively and can act as inhibitors to the virus precisely.[112] Ping et al. explored gFETs functionalized with probe DNA for

https://doi.org/10.1021/acsomega.2c01033
ACS Omega 2022, 7, 22073−22088

the fabrication of DNA biosensors effectively and scalably.[113] Chen et al. investigated an AlGaN/GaN high electron mobility transistor for miRNA identification that acted as an indicator and was highly selective for cardiovascular diseases.[114] Gao et al. fabricated nanoelectronic transistor sensors by 1D and 2D NMs.[115] A broad range of biological species was identified with high sensitivity. The researcher developed a gFET biosensor that was used for sensitive and selective recognition of *E. coli* with pyrene-DNA aptamer and exosome sensing.[116] Recently, a gFET-based biosensor was fabricated for a specific Ab against CoV-2 spike protein,[117] whereas Chen et al. found human mAb that blocked binding to the ACE2 receptor.[118]

Currently, 2D graphene has been used significantly in biosensing.[119−122] A magnetically controlled 2D nano-DNA fluorescence sensor was developed for detecting alkaline phosphatase, having a detection limit of 0.02 mU/mL. They utilized λ-exonuclease and a δ-FeOOH nanosheet, which possessed a fluorescence-quenching ability that differed with different DNA structures (ssDNA or dsDNA). Therefore, this sensor was comparatively better than the other 2D nano-DNA fluorescent sensors.[123,124] Further, the 3D graphene nanocomposite possessed a large surface area, biocompatibility, and electrical conductivity. These advantages attracted extensive interest in developing incensing and energy devices.[125,126] A one-step laser induction method was developed to prepare Au NP-3D graphene nanocomposites. They fabricated a flexible impedimetric immunosensor for *E. coli* detection, enhancing performance such as flexibility, sensitivity, and low detection limit.[125,127]

With the ongoing COVID-19 pandemic and the contagious nature of the HCoV-2, extreme protective measures are crucial to take while testing for COVID-19. The COVID-19 pandemic could be contained with the development of point-of-care diagnostic biosensors. However, due to restricted research practices, only certain laboratories could minimize COVID-19 spread, although development of point-of-care biosensors for accurate and sensitive diagnosis of COVID-19 could escalate specific testing that would limit the spread of infection.

Researchers also used an optomechanical device attached to a smartphone's camera to detect the viruses (Figure SI.18). The fluorescent imager on the smartphone had a laser diode with 450 nm excitation, a thin-film interference filter, a coarse numerical aperture lens, and a focusing and depth-adjustment coarse mechanical translation stage. A low-pass (LP) filter blocked the scattered excitation beam and formed a proficient background rejection mechanism to separate the very weak fluorescent signal that occurred from the viruses.[128]

5. CHALLENGES

A major challenge was concerned with the translation of research into commercial prototypes. Reliability of sensors, manufacturing protocols, and practical hands-on skills are fundamentally distant from each other and are limitations that need to be addressed. Automation might come up with solutions whereby rapid troubleshooting calibration is provided to users easily. Innovative biosensing technologies have future prospects in revolutionizing the healthcare system. There were ethical arguments like confidentiality, ownership, and privacy that were challenging to resolve in a short time frame, resulting in decreased technology adoption. The risks associated with self-use biosensors were unclear, and users were less inclined to read terms and conditions while using the applications. Still, laboratory-based testing eliminates ethical issues, and thus, exhaustive testing can be accomplished on sensing platforms. Therefore, biosensors and nanoscale visualization techniques can be encouraging tools, leading to a better understanding of pandemic strains. It can also provide on-site identification of viral strains for point-of-care prognosis and prevention of future pandemics at an early stage.[103] Despite several advantages of next-generation biosensors, only a limited number of NM-based biosensors are currently available. Therefore, further effort is critical for the widespread application of biosensors in the real world.

6. FUTURE PERSPECTIVES

Next-generation biosensors have gained significance in a wide range of applications across many interdisciplinary research areas. Pathogen detection is a very crucial aspect in healthcare management. However, available conventional approaches are bulky, expensive, and time-consuming, and only trained or skilled people can operate them. Hence, they are available at centralized laboratories.[129,130] Compared with the available diagnostic approaches, much attention has been given to electrochemical and FET biosensors because of miniaturization, point-of-care detection, on-site diagnosis, sensitivity, and low cost. Furthermore, multiplex biosensors could be developed for accurate detection of multiple biomarkers. Biosensors can ultimately lead to early diagnosis of COVID-19. Similarly, NP-based, smartphone-based, and wearable biosensors should be developed to control disease outbreak to contain human loss as early as possible.

Currently, a new horizon of NMO-based biosensors is established for clinical and non-clinical diagnosis. The exceptional properties of NMOs provide a huge scope for interdisciplinary research and have led researchers to establish interactions among several biomolecules−transducers using NMs. The possibility of developing biosensors based on NMOs for biomarkers, early detection, etc. is expected to be useful. To achieve enhanced charge transfer, fabrication of NMOs with desired groups may lead to the invention of a new approach for biosensor development. Also, the interface of NMO-based sensors could be utilized for real-time analyte monitoring.[131,132] The system can be extended to monitor public health, including constant recording and feedback approach, and can trace infections to ensure public health protection (Figure SI.19).[133] Functionalized NM-based biosensors may be used to detect bacteria in environmental and water resources. Moreover, functionalized biosensors can detect bacteria and heavy metals present in water resources.[134]

7. CONCLUSION

In this review, reports of various types of functionalized NMs used in the fabrication of different types of biosensors and prevalence in various biological and environmental monitoring in real time are discussed. Further, there is an emphasis on different types of biosensors and their unique properties, merits, and demerits. As illustrated, the integration of NMs has led to new perspectives in innovation of next-generation biosensors. Next-generation biosensors are prevalent in several areas of environmental monitoring such as detection of bacteria and pathogens present in environmental surroundings. Furthermore, an emphasis was given to biosensors' invention to curb the recent pandemic outbreak of nCoV and their utilization to control future pandemics similar to COVID-19.

https://doi.org/10.1021/acsomega.2c01033
ACS Omega 2022, 7, 22073−22088

■ ASSOCIATED CONTENT

Supporting Information

The Supporting Information is available free of charge at https://pubs.acs.org/doi/10.1021/acsomega.2c01033.

Brief on different applications, drug discovery, disease detection, cancer therapy, delivery system, molecular or optical imaging, optical biosensor, colorimetric detection, plasmonic biosensor, SWCNT-based biosensor, Au NP-based biosensors, UCNP-based biosensors, other materials-based biosensors, and utilization of biosensors in the detection of COVID-19 (PDF)

■ AUTHOR INFORMATION

Corresponding Authors

Akanksha Gupta − *Department of Chemistry, Sri Venkateswara College, University of Delhi, New Delhi, Delhi 110021, India*; Email: akankshachem05@gmail.com

Vinod Kumar − *Special Centre for Nanoscience, Jawaharlal Nehru University, New Delhi, Delhi 110067, India*; orcid.org/0000-0002-8362-8009; Email: kumarv@mail.jnu.ac.in

Authors

Sanjeev Kumar − *Department of Chemistry, University of Delhi, New Delhi, Delhi 110007, India; Department of Chemistry, Kirori Mal College, University of Delhi, New Delhi, Delhi 110007, India*

Ritika Sharma − *Department of Biochemistry, University of Delhi, New Delhi, Delhi 110021, India*

Bhawna − *Department of Chemistry, University of Delhi, New Delhi, Delhi 110007, India*

Prashant Singh − *Department of Chemistry, Atma Ram Sanatan Dharma College, University of Delhi, New Delhi, Delhi 110021, India*; orcid.org/0000-0001-9648-2275

Susheel Kalia − *Department of Chemistry, Indian Military Academy, Dehradun, Uttarakhand 248007, India*

Pankaj Thakur − *Special Centre for Nanoscience, Jawaharlal Nehru University, New Delhi, Delhi 110067, India*; orcid.org/0000-0003-0000-9411

Complete contact information is available at: https://pubs.acs.org/10.1021/acsomega.2c01033

Notes

The authors declare no competing financial interest.

■ ACKNOWLEDGMENTS

S.K. and Bhawna thank Council of Scientific & Industrial Research (File no. 08/694(0004)/2018-EMR-I) and University Grant Commission, respectively, for Senior Research Fellowship.

■ REFERENCES

(1) Sadeghi, P.; Sohrabi, H.; Hejazi, M.; Jahanban-Esfahlan, A.; Baradaran, B.; Tohidast, M.; Majidi, M. R.; Mokhtarzadeh, A.; Tavangar, S. M.; de la Guardia, M. Lateral flow assays (LFA) as an alternative medical diagnosis method for detection of virus species: The intertwine of nanotechnology with sensing strategies. *Trends Anal. Chem.* **2021**, *145*, 116460.

(2) Dai, Y.; Molazemhosseini, A.; Liu, C. C. A single-use, in vitro biosensor for the detection of t-tau protein, a biomarker of neurodegenerative disorders, in pbs and human serum using differential pulse voltammetry (DPV). *Biosensors* **2017**, *7* (1), 10.

(3) Chen, Y.; Ren, R.; Pu, H.; Guo, X.; Chang, J.; Zhou, G.; Mao, S.; Kron, M.; Chen, J. Field-effect transistor biosensor for rapid detection of Ebola antigen. *Sci. Rep.* **2017**, *7* (1), 10974.

(4) García-Rubio, D. L.; de la Mora, M.; Cerecedo, D.; Saniger Blesa, J. M.; Villagrán-Muniz, M. An optical-based biosensor of the epithelial sodium channel as a tool for diagnosing hypertension. *Biosens. Bioelectron.* **2020**, *157*, 112151.

(5) Koo, B.; Kim, D.-e.; Kweon, J.; Jin, C. E.; Kim, S.-H.; Kim, Y.; Shin, Y. CRISPR/dCas9-mediated biosensor for detection of tick-borne diseases. *Sens. Actuators B Chem.* **2018**, *273*, 316−321.

(6) Jayanthi, V. S. A.; Das, A. B.; Saxena, U. Recent advances in biosensor development for the detection of cancer biomarkers. *Biosens. Bioelectron.* **2017**, *91*, 15−23.

(7) Salek-Maghsoudi, A.; Vakhshiteh, F.; Torabi, R.; Hassani, S.; Ganjali, M. R.; Norouzi, P.; Hosseini, M.; Abdollahi, M. Recent advances in biosensor technology in assessment of early diabetes biomarkers. *Biosens. Bioelectron.* **2018**, *99*, 122−135.

(8) Schmidt-Speicher, L. M.; Länge, K. Microfluidic Integration for Electrochemical Biosensor Applications. *Curr. Opin. Electrochem.* **2021**, *29*, 100755.

(9) Hemaja, V.; Panda, D. K. A comprehensive review on high electron mobility transistor (HEMT) Based biosensors: recent advances and future prospects and its comparison with Si-based biosensor. *Silicon* **2022**, *14*, 1873−1886.

(10) Serrano, P. C.; Nunes, G. E.; Avila, L. B.; Reis, C. P.; Gomes, A.; Reis, F. T.; Sartorelli, M. L.; Melegari, S. P.; Matias, W. G.; Bechtold, I. H. Electrochemical impedance biosensor for detection of saxitoxin in aqueous solution. *Anal. Bioanal. Chem.* **2021**, *413*, 6393−6399.

(11) Nagraik, R.; Sharma, A.; Kumar, D.; Chawla, P.; Kumar, A. P. Milk adulterant detection: Conventional and biosensor based approaches: A review. *Sens. Bio-Sens. Res.* **2021**, *33*, 100433.

(12) Yoon, J.; Shin, M.; Lee, T.; Choi, J.-W. Highly sensitive biosensors based on biomolecules and functional nanomaterials depending on the types of nanomaterials: A perspective review. *Mater.* **2020**, *13* (2), 299.

(13) Yoo, S. M.; Lee, S. Y. Optical biosensors for the detection of pathogenic microorganisms. *Trends Biotechnol.* **2016**, *34* (1), 7−25.

(14) Li, D.; Chen, H.; Fan, K.; Labunov, V.; Lazarouk, S.; Yue, X.; Liu, C.; Yang, X.; Dong, L.; Wang, G. A supersensitive silicon nanowire array biosensor for quantitating tumor marker ctDNA. *Biosens. Bioelectron.* **2021**, *181*, 113147.

(15) Zhu, Q.; Liu, L.; Wang, R.; Zhou, X. A split aptamer (SPA)-based sandwich-type biosensor for facile and rapid detection of streptomycin. *J. Hazard. Mater.* **2021**, *403*, 123941.

(16) Cooper, M. A. Optical biosensors in drug discovery. *Nat. Rev. Drug Discovery* **2002**, *1* (7), 515−528.

(17) Lai, M.; Slaughter, G. Label-free MicroRNA optical biosensors. *Nanomaterials* **2019**, *9* (11), 1573.

(18) Du, H.; Li, Z.; Wang, Y.; Yang, Q.; Wu, W. Nanomaterial-based optical biosensors for the detection of foodborne bacteria. *Food Rev. Int.* **2020**, 1−30.

(19) Eveness, J.; Cao, L.; Kiely, J.; Luxton, R. Equivalent circuit model of a non-faradaic impedimetric ZnO nano-crystal biosensor. *J. Electroanal. Chem.* **2022**, *906*, 116003.

(20) Zhu, Z.; Yasui, T.; Liu, Q.; Nagashima, K.; Takahashi, T.; Shimada, T.; Yanagida, T.; Baba, Y. J. M. Fabrication of a Robust In2O3 Nanolines FET Device as a Biosensor Platform. *Micromachines* **2021**, *12* (6), 642.

(21) Arlett, J.; Myers, E.; Roukes, M. Comparative advantages of mechanical biosensors. *Nat. Nanotechnol.* **2011**, *6* (4), 203−215.

(22) Zhang, H.; Fan, G.; Li, S.; Cai, X.; Wei, J.; Jing, G.; Li, Y.; Zhang, Z. J. J. o. M. Integrated Opto-mechanical Cantilever Sensor with a Rib Waveguide. *J. Microsc.* **2022**, *286*, 240.

(23) Zhang, Q.; Dong, Z.; Dong, X.; Duan, Q.; Ji, J.; Liu, Y.; Pei, Z.; Ji, C.; Sang, S. J. A. M. I. Double-Side-Coated Grid-Type Mechanical Membrane Biosensor Based on AuNPs Self-assembly and 3D Printing. *Adv. Mater. Interfaces* **2022**, *9* (3), 2101461.

(24) Cui, L.; Li, Y.; Lu, M.; Tang, B.; Zhang, C.-y. An ultrasensitive electrochemical biosensor for polynucleotide kinase assay based on gold nanoparticle-mediated lambda exonuclease cleavage-induced signal amplification. *Biosens. Bioelectron.* **2018**, *99*, 1−7.
(25) Jia, X.; Dong, S.; Wang, E. Engineering the bioelectrochemical interface using functional nanomaterials and microchip technique toward sensitive and portable electrochemical biosensors. *Biosens. Bioelectron.* **2016**, *76*, 80−90.
(26) Elbadawi, M.; Ong, J. J.; Pollard, T. D.; Gaisford, S.; Basit, A. W. Additive manufacturable materials for electrochemical biosensor electrodes. *Adv. Funct. Mater.* **2021**, *31* (10), 2006407.
(27) He, L.; Huang, R.; Xiao, P.; Liu, Y.; Jin, L.; Liu, H.; Li, S.; Deng, Y.; Chen, Z.; Li, Z.; He, N. Current signal amplification strategies in aptamer-based electrochemical biosensor: A review. *Chin. Chem. Lett.* **2021**, *32*, 1593−1602.
(28) Samani, S. S.; Khojastehnezhad, A.; Ramezani, M.; Alibolandi, M.; Yazdi, F. T.; Mortazavi, S. A.; Khoshbin, Z.; Abnous, K.; Taghdisi, S. M. Ultrasensitive detection of micrococcal nuclease activity and Staphylococcus aureus contamination using optical biosensor technology-A review. *Talanta* **2021**, *226*, 122168.
(29) Ma, J.; Du, Y.; Jiang, Y.; Shen, L.; Ma, H.; Lv, F.; Cui, Z.; Pan, Y.; Shi, L.; Zhu, N. Wearable healthcare smart electrochemical biosensors based on co-assembled prussian blue—graphene film for glucose sensing. *Mikrochim. Acta* **2022**, *189* (1), 46.
(30) Yu, Y.; Nassar, J.; Xu, C.; Min, J.; Yang, Y.; Dai, A.; Doshi, R.; Huang, A.; Song, Y.; Gehlhar, R. J. S. r. Biofuel-powered soft electronic skin with multiplexed and wireless sensing for human-machine interfaces. *Sci. Rob.* **2020**, *5* (41), eaaz7946.
(31) Wang, B.; Cao, J.-T.; Liu, Y.-M. Recent progress of heterostructure-based photoelectrodes in photoelectrochemical biosensing: a mini review. *Analyst* **2020**, *145* (4), 1121−1128.
(32) Devadoss, A.; Sudhagar, P.; Terashima, C.; Nakata, K.; Fujishima, A. Photoelectrochemical biosensors: New insights into promising photoelectrodes and signal amplification strategies. *J. Photochem. Photobiol. C* **2015**, *24*, 43−63.
(33) Zhao, J.; Fu, C.; Huang, C.; Zhang, S.; Wang, F.; Zhang, Y.; Zhang, L.; Ge, S.; Yu, J. Co3O4-Au polyhedron mimic peroxidase-and cascade enzyme-assisted cycling process-based photoelectrochemical biosensor for monitoring of miRNA-141. *Chem. Eng. J.* **2021**, *406*, 126892.
(34) Yang, J.; Li, Y.; Guo, L.; Qiu, B.; Lin, Z. J. A. c. Photoelectrochemical Biosensor for MicroRNA-21 Based on High Photocurrent of TiO2/Two-Dimensional Coordination Polymer CuCl x (MBA) y Photoelectrode. *Anal. Chem.* **2021**, *93* (31), 11010−11018.
(35) Kumar, V.; Choudhary, A. K.; Kumar, P.; Sharma, S. Nanotechnology: nanomedicine, nanotoxicity and future challenges. *Nanosci. Nanotechnol. - Asia* **2018**, *9* (1), 64−78.
(36) Dervisevic, M.; Dervisevic, E.; Şenel, M. Recent progress in nanomaterial-based electrochemical and optical sensors for hypoxanthine and xanthine. A review. *Microchimica Acta* **2019**, *186* (12), 749.
(37) Cao, S.-P.; Hu, H.-M.; Liang, R.-P.; Qiu, J.-D. An ultrasensitive electrochemiluminescence resonance energy transfer biosensor for divalent mercury monitoring. *J. Electroanal. Chem.* **2020**, *856*, 113494.
(38) Chen, D.; Lv, L.; Peng, L.; Peng, J.; Cao, Y.; Wang, X.; Wang, X.; Wu, Q.; Tu, J. Controlled synthesis of mesoporous zinc oxide containing oxygen vacancies in low annealing temperature for photoelectrochemical biosensor. *Ceram. Int.* **2019**, *45* (14), 18044−18051.
(39) Alim, S.; Kafi, A.; Rajan, J.; Yusoff, M. M. Application of polymerized multiporous nanofiber of SnO2 for designing a bienzyme glucose biosensor based on HRP/GOx. *Int. J. Biol. Macromol.* **2019**, *123*, 1028−1034.
(40) Faria, A. M.; Mazon, T. Early diagnosis of Zika infection using a ZnO nanostructures-based rapid electrochemical biosensor. *Talanta* **2019**, *203*, 153−160.
(41) Şerban, I.; Enesca, A. Metal Oxides-Based Semiconductors for Biosensors Applications. *Front. Chem.* **2020**, *8*, 354.
(42) Rahman, M.; Ahammad, A.; Jin, J.-H.; Ahn, S. J.; Lee, J.-J. A comprehensive review of glucose biosensors based on nanostructured metal-oxides. *Sensors* **2010**, *10* (5), 4855−4886.
(43) Solanki, P. R.; Kaushik, A.; Agrawal, V. V.; Malhotra, B. D. Nanostructured metal oxide-based biosensors. *NPG Asia Materials* **2011**, *3* (1), 17−24.
(44) Yoon, J.; Lee, S. N.; Shin, M. K.; Kim, H.-W.; Choi, H. K.; Lee, T.; Choi, J.-W. Flexible electrochemical glucose biosensor based on GOx/gold/MoS2/gold nanofilm on the polymer electrode. *Biosens. Bioelectron.* **2019**, *140*, 111343.
(45) Gu, H.; Xing, Y.; Xiong, P.; Tang, H.; Li, C.; Chen, S.; Zeng, R.; Han, K.; Shi, G. Three-Dimensional Porous Ti3C2T x MXene-Graphene Hybrid Films for Glucose Biosensing. *ACS Appl. Nano Mater.* **2019**, *2* (10), 6537−6545.
(46) Kong, T.; Chen, Y.; Ye, Y.; Zhang, K.; Wang, Z.; Wang, X. An amperometric glucose biosensor based on the immobilization of glucose oxidase on the ZnO nanotubes. *Sens. Actuators B Chem.* **2009**, *138* (1), 344−350.
(47) Liu, J.; Li, Y.; Huang, X.; Zhu, Z. Tin oxide nanorod array-based electrochemical hydrogen peroxide biosensor. *Nanoscale Res. Lett.* **2010**, *5* (7), 1177−1181.
(48) Saha, S.; Arya, S. K.; Singh, S.; Sreenivas, K.; Malhotra, B.; Gupta, V. Nanoporous cerium oxide thin film for glucose biosensor. *Biosens. Bioelectron.* **2009**, *24* (7), 2040−2045.
(49) Kaushik, A.; Khan, R.; Solanki, P. R.; Pandey, P.; Alam, J.; Ahmad, S.; Malhotra, B. Iron oxide nanoparticles-chitosan composite based glucose biosensor. *Biosens. Bioelectron.* **2008**, *24* (4), 676−683.
(50) Salimi, A.; Sharifi, E.; Noorbakhsh, A.; Soltanian, S. Immobilization of glucose oxidase on electrodeposited nickel oxide nanoparticles: direct electron transfer and electrocatalytic activity. *Biosens. Bioelectron.* **2007**, *22* (12), 3146−3153.
(51) Zhang, W.; Yang, T.; Huang, D. M.; Jiao, K. Electrochemical sensing of DNA immobilization and hybridization based on carbon nanotubes/nano zinc oxide/chitosan composite film. *Chin. Chem. Lett.* **2008**, *19* (5), 589−591.
(52) Tan, L.; Chen, Y.; Yang, H.; Shi, Y.; Si, J.; Yang, G.; Wu, Z.; Wang, P.; Lu, X.; Bai, H.; et al. Alpha-1-fetoprotein antibody functionalized Au nanoparticles: Catalytic labels for the electrochemical detection of α-1-fetoprotein based on TiO2 nanoparticles synthesized with ionic liquid. *Sens. Actuators B Chem.* **2009**, *142* (1), 316−320.
(53) Che, X.; Yuan, R.; Chai, Y.; Li, J.; Song, Z.; Wang, J. Amperometric immunosensor for the determination of α-1-fetoprotein based on multiwalled carbon nanotube-silver nanoparticle composite. *J. Colloid Interface Sci.* **2010**, *345* (2), 174−180.
(54) Wang, Q.; Jiang, X.; Niu, L.-Y.; Fan, X.-C. Enhanced sensitivity of bimetallic optical fiber SPR sensor based on MoS2 nanosheets. *Opt. Lasers Eng.* **2020**, *128*, 105997.
(55) Gupta, P. K.; Chauhan, D.; Khan, Z. H.; Solanki, P. R. ZrO2 Nanoflowers Decorated with Graphene Quantum Dots for Electrochemical Immunosensing. *ACS Appl. Nano Mater.* **2020**, *3* (3), 2506−2516.
(56) Zhang, Y.; Xu, Y.; Li, Z.; Chen, T.; Lantz, S. M.; Howard, P. C.; Paule, M. G.; Slikker Jr, W.; Watanabe, F.; Mustafa, T.; et al. Mechanistic toxicity evaluation of uncoated and PEGylated single-walled carbon nanotubes in neuronal PC12 cells. *ACS Nano* **2011**, *5* (9), 7020−7033.
(57) Bhirde, A. A.; Patel, S.; Sousa, A. A.; Patel, V.; Molinolo, A. A.; Ji, Y.; Leapman, R. D.; Gutkind, J. S.; Rusling, J. F. Distribution and clearance of PEG-single-walled carbon nanotube cancer drug delivery vehicles in mice. *Nanomedicine* **2010**, *5* (10), 1535−1546.
(58) Yan, X.-B.; Gu, Y.-H.; Huang, D.; Gan, L.; Wu, L.-X.; Huang, L.-H.; Chen, Z.-D.; Huang, S.-P.; Zhou, K.-C. Binding tendency with oligonucleotides and cell toxicity of cetyltrimethyl ammonium bromide-coated single-walled carbon nanotubes. *Trans. Nonferrous Met. Soc. China* **2011**, *21* (5), 1085−1091.
(59) Krajcik, R.; Jung, A.; Hirsch, A.; Neuhuber, W.; Zolk, O. Functionalization of carbon nanotubes enables non-covalent binding and intracellular delivery of small interfering RNA for efficient knock-

https://doi.org/10.1021/acsomega.2c01033
ACS Omega 2022, 7, 22073−22088

down of genes. *Biochem. Biophys. Res. Commun.* **2008**, *369* (2), 595−602.
(60) Ge, C.; Du, J.; Zhao, L.; Wang, L.; Liu, Y.; Li, D.; Yang, Y.; Zhou, R.; Zhao, Y.; Chai, Z.; et al. Binding of blood proteins to carbon nanotubes reduces cytotoxicity. *Proc. Natl. Acad. Sci. U. S. A.* **2011**, *108* (41), 16968−16973.
(61) Kam, N. W. S.; Liu, Z.; Dai, H. Functionalization of carbon nanotubes via cleavable disulfide bonds for efficient intracellular delivery of siRNA and potent gene silencing. *J. Am. Chem. Soc.* **2005**, *127* (36), 12492−12493.
(62) Singh, R.; Pantarotto, D.; McCarthy, D.; Chaloin, O.; Hoebeke, J.; Partidos, C. D.; Briand, J.-P.; Prato, M.; Bianco, A.; Kostarelos, K. Binding and condensation of plasmid DNA onto functionalized carbon nanotubes: toward the construction of nanotube-based gene delivery vectors. *J. Am. Chem. Soc.* **2005**, *127* (12), 4388−4396.
(63) Chen, J.; Chen, S.; Zhao, X.; Kuznetsova, L. V.; Wong, S. S.; Ojima, I. Functionalized single-walled carbon nanotubes as rationally designed vehicles for tumor-targeted drug delivery. *J. Am. Chem. Soc.* **2008**, *130* (49), 16778−16785.
(64) Karimi-Maleh, H.; Alizadeh, M.; Orooji, Y.; Karimi, F.; Baghayeri, M.; Rouhi, J.; Tajik, S.; Beitollahi, H.; Agarwal, S.; Gupta, V. K.; et al. Guanine-based DNA biosensor amplified with Pt/SWCNTs nanocomposite as analytical tool for nanomolar determination of daunorubicin as an anticancer drug: a docking/experimental investigation. *Ind. Eng. Chem. Res.* **2021**, *60* (2), 816−823.
(65) Ahmed, J.; Rashed, M. A.; Faisal, M.; Harraz, F. A.; Jalalah, M.; Alsareii, S. Novel SWCNTs-mesoporous silicon nanocomposite as efficient non-enzymatic glucose biosensor. *Appl. Surf. Sci.* **2021**, *552*, 149477.
(66) Tao, L.; Chen, G.; Mantovani, G.; York, S.; Haddleton, D. M. Modification of multi-wall carbon nanotube surfaces with poly (amidoamine) dendrons: synthesis and metal templating. *Chem. Commun.* **2006**, No. 47, 4949−4951.
(67) Yu, B.-Z.; Ma, J.-F.; Li, W.-X. Polyethylenimine-modified multiwalled carbon nanotubes for plasmid DNA gene delivery. *Nat. Preced.* **2009**, 1.
(68) Xu, L.; Liu, Y.; Chen, Z.; Li, W.; Liu, Y.; Wang, L.; Liu, Y.; Wu, X.; Ji, Y.; Zhao, Y.; et al. Surface-engineered gold nanorods: promising DNA vaccine adjuvant for HIV-1 treatment. *Nano Lett.* **2012**, *12* (4), 2003−2012.
(69) Lee, T.; Mohammadniaei, M.; Zhang, H.; Yoon, J.; Choi, H. K.; Guo, S.; Guo, P.; Choi, J. W. Single Functionalized pRNA/Gold Nanoparticle for Ultrasensitive MicroRNA Detection Using Electrochemical Surface-Enhanced Raman Spectroscopy. *Adv. Sci.* **2020**, *7* (3), 1902477.
(70) Hwu, S.; Garzuel, M.; Forró, C.; Ihle, S. J.; Reichmuth, A. M.; Kurdzesau, F.; Vörös, J. An analytical method to control the surface density and stability of DNA-gold nanoparticles for an optimized biosensor. *Colloids Surf. B. Biointerfaces* **2020**, *187*, 110650.
(71) Zhou, S.; Gan, Y.; Kong, L.; Sun, J.; Liang, T.; Wang, X.; Wan, H.; Wang, P. A novel portable biosensor based on aptamer functionalized gold nanoparticles for adenosine detection. *Anal. Chim. Acta* **2020**, *1120*, 43−49.
(72) Steinmetz, M.; Lima, D.; Viana, A. G.; Fujiwara, S. T.; Pessôa, C. A.; Etto, R. M.; Wohnrath, K. A sensitive label-free impedimetric DNA biosensor based on silsesquioxane-functionalized gold nanoparticles for Zika Virus detection. *Biosens. Bioelectron.* **2019**, *141*, 111351.
(73) Bai, W.; Wei, Y.; Zhang, Y.; Bao, L.; Li, Y. Label-free and amplified electrogenerated chemiluminescence biosensing for the detection of thymine DNA glycosylase activity using DNA-functionalized gold nanoparticles triggered hybridization chain reaction. *Anal. Chim. Acta* **2019**, *1061*, 101−109.
(74) Huang, J.; Zhang, Y.; Lin, Z.; Liu, W.; Chen, X.; Liu, Y.; Tian, H.; Liu, Q.; Gillibert, R.; Spadavecchia, J.; et al. Femtomolar detection of nucleic acid based on functionalized gold nanoparticles. *Nanophotonics* **2019**, *8* (9), 1495−1503.
(75) Mohammed, A. S.; Nagarjuna, R.; Khaja, M. N.; Ganesan, R.; Ray Dutta, J. Effects of free patchy ends in ssDNA and dsDNA on gold nanoparticles in a colorimetric gene sensor for Hepatitis C virus RNA. *Microchimica Acta* **2019**, *186* (8), 566.
(76) Wang, H.; Tang, H.; Yang, C.; Li, Y. Selective single molecule nanopore sensing of microRNA using PNA functionalized magnetic core-shell Fe3O4-Au nanoparticles. *Anal. Chem.* **2019**, *91* (12), 7965−7970.
(77) Gao, X.; Zhu, Y.; Zhao, X.; Wang, Z.; An, D.; Ma, Y.; Guan, S.; Du, Y.; Zhou, B. Synthesis and characterization of polyurethane/SiO2 nanocomposites. *Appl. Surf. Sci.* **2011**, *257* (10), 4719−4724.
(78) Naka, Y.; Komori, Y.; Yoshitake, H. One-pot synthesis of organo-functionalized monodisperse silica particles in W/O microemulsion and the effect of functional groups on addition into polystyrene. *Colloids Surf. Physicochem. Eng. Aspects* **2010**, *361* (1−3), 162−168.
(79) Zhou, W.-J.; Chen, Y.; Corn, R. M. Ultrasensitive microarray detection of short RNA sequences with enzymatically modified nanoparticles and surface plasmon resonance imaging measurements. *Anal. Chem.* **2011**, *83* (10), 3897−3902.
(80) Lahiri, D.; Rouzaud, F.; Richard, T.; Keshri, A. K.; Bakshi, S. R.; Kos, L.; Agarwal, A. Boron nitride nanotube reinforced polylactide-polycaprolactone copolymer composite: Mechanical properties and cytocompatibility with osteoblasts and macrophages in vitro. *Acta Biomater.* **2010**, *6* (9), 3524−3533.
(81) Ciofani, G.; Raffa, V.; Menciassi, A.; Cuschieri, A. Cytocompatibility, interactions, and uptake of polyethyleneimine-coated boron nitride nanotubes by living cells: Confirmation of their potential for biomedical applications. *Biotechnol. Bioeng.* **2008**, *101* (4), 850−858.
(82) Emanet, M.; Şen, Ö.; Çobandede, Z.; Çulha, M. Interaction of carbohydrate modified boron nitride nanotubes with living cells. *Colloids Surf. B. Biointerfaces* **2015**, *134*, 440−446.
(83) Ciofani, G.; Danti, S.; Nitti, S.; Mazzolai, B.; Mattoli, V.; Giorgi, M. Biocompatibility of boron nitride nanotubes: an up-date of in vivo toxicological investigation. *Int. J. Pharm.* **2013**, *444* (1−2), 85−88.
(84) Jiang, S.; Zhang, Y.; Lim, K. M.; Sim, E. K.; Ye, L. NIR-to-visible upconversion nanoparticles for fluorescent labeling and targeted delivery of siRNA. *Nanotechnology* **2009**, *20* (15), 155101.
(85) Mi, C.; Zhang, J.; Gao, H.; Wu, X.; Wang, M.; Wu, Y.; Di, Y.; Xu, Z.; Mao, C.; Xu, S. Multifunctional nanocomposites of superparamagnetic (Fe 3 O 4) and NIR-responsive rare earth-doped up-conversion fluorescent (NaYF 4: Yb, Er) nanoparticles and their applications in biolabeling and fluorescent imaging of cancer cells. *Nanoscale* **2010**, *2* (7), 1141−1148.
(86) Yuan, P.; Lee, Y. H.; Gnanasammandhan, M. K.; Guan, Z.; Zhang, Y.; Xu, Q.-H. Plasmon enhanced upconversion luminescence of NaYF4: Yb, Er@ SiO 2@ Ag core-shell nanocomposites for cell imaging. *Nanoscale* **2012**, *4* (16), 5132−5137.
(87) Chen, Z.; Chen, H.; Hu, H.; Yu, M.; Li, F.; Zhang, Q.; Zhou, Z.; Yi, T.; Huang, C. Versatile synthesis strategy for carboxylic acid-functionalized upconverting nanophosphors as biological labels. *J. Am. Chem. Soc.* **2008**, *130* (10), 3023−3029.
(88) Wilhelm, S.; Hirsch, T.; Patterson, W. M.; Scheucher, E.; Mayr, T.; Wolfbeis, O. S. Multicolor upconversion nanoparticles for protein conjugation. *Theranostics* **2013**, *3* (4), 239.
(89) Nagarajan, S.; Li, Z.; Marchi-Artzner, V.; Grasset, F.; Zhang, Y. Imaging gap junctions with silica-coated upconversion nanoparticles. *Med. Biol. Eng. Comput* **2010**, *48* (10), 1033−1041.
(90) Yang, L.; Wang, H.; Lü, H.; Hui, N. Phytic Acid Functionalized Antifouling Conducting Polymer Hydrogel for Electrochemical Detection of MicroRNA. *Anal. Chim. Acta* **2020**, *1124*, 104−112.
(91) Fan, J.; Zang, Y.; Jiang, J.; Lei, J.; Xue, H. Beta-cyclodextrin-functionalized CdS nanorods as building modules for ultrasensitive photoelectrochemical bioassay of HIV DNA. *Biosens. Bioelectron.* **2019**, *142*, 111557.
(92) Wang, J.; Hui, N. Electrochemical functionalization of polypyrrole nanowires for the development of ultrasensitive biosensors for detecting microRNA. *Sens. Actuators B Chem.* **2019**, *281*, 478−485.

https://doi.org/10.1021/acsomega.2c01033
ACS Omega 2022, 7, 22073−22088

(93) Rohilla, D.; Chaudhary, S.; Kaur, N.; Shanavas, A. Dopamine functionalized CuO nanoparticles: A high valued "turn on" colorimetric biosensor for detecting cysteine in human serum and urine samples. *Mater. Sci. Eng., C* **2020**, *110*, 110724.
(94) Chauhan, D.; Kumar, R.; Panda, A. K.; Solanki, P. R. An efficient electrochemical biosensor for Vitamin-D3 detection based on aspartic acid functionalized gadolinium oxide nanorods. *J. Mater. Res. Technol.* **2019**, *8* (6), 5490−5503.
(95) Ou, X.; Pu, Q.; Sheng, S.; Dai, T.; Gou, D.; Yu, W.; Yang, T.; Dai, L.; Yang, Y.; Xie, G. Electrochemical competitive immunodetection of messenger RNA modified with N6-methyladenosine by using DNA-modified mesoporous PtCo nanospheres. *Microchim. Acta* **2020**, *187* (1), 31.
(96) Yang, Z.; Yi, C.; Lv, S.; Sheng, Y.; Wen, W.; Zhang, X.; Wang, S. Development of a lateral flow strip biosensor based on copper oxide nanoparticles for rapid and sensitive detection of HPV16 DNA. *Sens. Actuators B Chem.* **2019**, *285*, 326−332.
(97) Li, H.; Lin, H.; Lv, W.; Gai, P.; Li, F. Equipment-free and visual detection of multiple biomarkers via an aggregation induced emission luminogen-based paper biosensor. *Biosens. Bioelectron.* **2020**, *165*, 112336.
(98) Sheng, Y.; Zhang, T.; Zhang, S.; Johnston, M.; Zheng, X.; Shan, Y.; Liu, T.; Huang, Z.; Qian, F.; Xie, Z.; et al. A CRISPR/Cas13a-powered catalytic electrochemical biosensor for successive and highly sensitive RNA diagnostics. *Biosens. Bioelectron.* **2021**, *178*, 113027.
(99) Zeng, R.; Wang, W.; Chen, M.; Wan, Q.; Wang, C.; Knopp, D.; Tang, D. CRISPR-Cas12a-driven MXene-PEDOT: PSS piezoresistive wireless biosensor. *Nano Energy* **2021**, *82*, 105711.
(100) Marras, S. A. Selection of fluorophore and quencher pairs for fluorescent nucleic acid hybridization probes. In *Fluorescent energy transfer nucleic acid probes*; Springer: 2006; pp 3−16.
(101) Yakoh, A.; Pimpitak, U.; Rengpipat, S.; Hirankarn, N.; Chailapakul, O.; Chaiyo, S. based electrochemical biosensor for diagnosing COVID-19: Detection of SARS-CoV-2 antibodies and antigen. *Biosens. Bioelectron.* **2021**, *176*, 112912.
(102) Schmidt, N.; Lareau, C. A.; Keshishian, H.; Ganskih, S.; Schneider, C.; Hennig, T.; Melanson, R.; Werner, S.; Wei, Y.; Zimmer, M.; et al. The SARS-CoV-2 RNA-protein interactome in infected human cells. *Nat. Microbiol.* **2021**, *6* (3), 339−353.
(103) Bhalla, N.; Pan, Y.; Yang, Z.; Payam, A. F. Opportunities and challenges for biosensors and nanoscale analytical tools for pandemics: COVID-19. *ACS Nano* **2020**, *14* (7), 7783−7807.
(104) Hornuss, D.; Lange, B.; Schröter, N.; Rieg, S.; Kern, W. V.; Wagner, D. Anosmia in COVID-19 patients. *Clin. Microbiol. Infect.* **2020**, *26*, 1426−1427.
(105) Bowman, G. L. *Biomarkers for early detection of Parkinson disease: a scent of consistency with olfactory dysfunction*; AAN Enterprises: 2017.
(106) Miripour, Z. S.; Sarrami-Forooshani, R.; Sanati, H.; Makarem, J.; Taheri, M. S.; Shojaeian, F.; Eskafi, A. H.; Abbasvandi, F.; Namdar, N.; Ghafari, H.; et al. Real-time diagnosis of reactive oxygen species (ROS) in fresh sputum by electrochemical tracing; correlation between COVID-19 and viral-induced ROS in lung/respiratory epithelium during this pandemic. *Biosens. Bioelectron.* **2020**, *165*, 112435.
(107) Asif, M.; Ajmal, M.; Ashraf, G.; Muhammad, N.; Aziz, A.; Iftikhar, T.; Wang, J.; Liu, H. The role of biosensors in COVID-19 outbreak. *Curr. Opin. Electrochem.* **2020**, *23*, 174−184.
(108) Kerry, R. G.; Malik, S.; Redda, Y. T.; Sahoo, S.; Patra, J. K.; Majhi, S. Nano-based approach to combat emerging viral (NIPAH virus) infection. *Nanomed. Nanotechnol. Biol. Med.* **2019**, *18*, 196−220.
(109) Zhu, H.; Fohlerová, Z.; Pekárek, J.; Basova, E.; Neužil, P. Recent advances in lab-on-a-chip technologies for viral diagnosis. *Biosens. Bioelectron.* **2020**, *153*, 112041.
(110) Mokhtarzadeh, A.; Eivazzadeh-Keihan, R.; Pashazadeh, P.; Hejazi, M.; Gharaatifar, N.; Hasanzadeh, M.; Baradaran, B.; de la Guardia, M. Nanomaterial-based biosensors for detection of pathogenic virus. *TrAC, Trends Anal. Chem.* **2017**, *97*, 445−457.
(111) Hwang, M. T.; Heiranian, M.; Kim, Y.; You, S.; Leem, J.; Taqieddin, A.; Faramarzi, V.; Jing, Y.; Park, I.; van der Zande, A. M.; et al. Ultrasensitive detection of nucleic acids using deformed graphene channel field effect biosensors. *Nat. Commun.* **2020**, *11*, 1543.
(112) Roh, C. A facile inhibitor screening of hepatitis C virus NS3 protein using nanoparticle-based RNA. *Biosensors* **2012**, *2* (4), 427−432.
(113) Ping, J.; Vishnubhotla, R.; Vrudhula, A.; Johnson, A. C. Scalable production of high-sensitivity, label-free DNA biosensors based on back-gated graphene field effect transistors. *ACS Nano* **2016**, *10* (9), 8700−8704.
(114) Chen, Y.-W.; Kuo, W.-C.; Tai, T.-Y.; Hsu, C.-P.; Sarangadharan, I.; Pulikkathodi, A. K.; Wang, S.-L.; Sukesan, R.; Lin, H.-Y.; Kao, K.-W.; et al. Highly sensitive and rapid MicroRNA detection for cardiovascular diseases with electrical double layer (EDL) gated AlGaN/GaN high electron mobility transistors. *Sens. Actuators B Chem.* **2018**, *262*, 365−370.
(115) Gao, N.; Gao, T.; Yang, X.; Dai, X.; Zhou, W.; Zhang, A.; Lieber, C. M. Specific detection of biomolecules in physiological solutions using graphene transistor biosensors. *Proc. Natl. Acad. Sci. U. S. A.* **2016**, *113* (51), 14633−14638.
(116) Kwong Hong Tsang, D.; Lieberthal, T. J.; Watts, C.; Dunlop, I. E.; Ramadan, S.; del Rio Hernandez, A. E.; Klein, N. Chemically Functionalised Graphene FET Biosensor for the Label-free Sensing of Exosomes. *Sci. Rep.* **2019**, *9*, 13946.
(117) Seo, G.; Lee, G.; Kim, M. J.; Baek, S.-H.; Choi, M.; Ku, K. B.; Lee, C.-S.; Jun, S.; Park, D.; Kim, H. G. Rapid Detection of COVID-19 Causative Virus (SARS-CoV-2) in Human Nasopharyngeal Swab Specimens Using Field-Effect Transistor-Based Biosensor. *ACS Nano* **2020**, *14*, 5135.
(118) Chen, X.; Li, R.; Pan, Z.; Qian, C.; Yang, Y.; You, R.; Zhao, J.; Liu, P.; Gao, L.; Li, Z.; et al. Human monoclonal antibodies block the binding of SARS-CoV-2 spike protein to angiotensin converting enzyme 2 receptor. *Cell. Mol. Immunol.* **2020**, *17*, 647−649.
(119) Li, X.; Fu, Y.; Ding, X.; Li, Z.; Zhu, G.; Fan, J. Magnetically controlled 2D nano-DNA fluorescent biosensor for selective and sensitive detection of alkaline phosphatase activity. *Sens. Actuators B Chem.* **2021**, *327*, 128914.
(120) Nong, J.; Lan, G.; Jin, W.; Luo, P.; Guo, C.; Tang, X.; Zang, Z.; Wei, W. Eco-friendly and high-performance photoelectrochemical anode based on AgInS 2 quantum dots embedded in 3D graphene nanowalls. *J. Mater. Chem. C* **2019**, *7* (32), 9830−9839.
(121) Chen, Y.; Tan, C.; Zhang, H.; Wang, L. Two-dimensional graphene analogues for biomedical applications. *Chem. Soc. Rev.* **2015**, *44* (9), 2681−2701.
(122) Mo, L.; Li, J.; Liu, Q.; Qiu, L.; Tan, W. Nucleic acid-functionalized transition metal nanosheets for biosensing applications. *Biosens. Bioelectron.* **2017**, *89*, 201−211.
(123) Wei, J.; Zang, Z.; Zhang, Y.; Wang, M.; Du, J.; Tang, X. Enhanced performance of light-controlled conductive switching in hybrid cuprous oxide/reduced graphene oxide (Cu 2 O/rGO) nanocomposites. *Opt. Lett.* **2017**, *42* (5), 911−914.
(124) Liu, X.; Xu, T.; Li, Y.; Zang, Z.; Peng, X.; Wei, H.; Zha, W.; Wang, F. Enhanced X-ray photon response in solution-synthesized CsPbBr3 nanoparticles wrapped by reduced graphene oxide. *Sol. Energy Mater. Sol. Cells* **2018**, *187*, 249−254.
(125) You, Z.; Qiu, Q.; Chen, H.; Feng, Y.; Wang, X.; Wang, Y.; Ying, Y. Laser-induced noble metal nanoparticle-graphene composites enabled flexible biosensor for pathogen detection. *Biosens. Bioelectron.* **2020**, *150*, 111896.
(126) Qiu, B.; Xing, M.; Zhang, J. Recent advances in three-dimensional graphene based materials for catalysis applications. *Chem. Soc. Rev.* **2018**, *47* (6), 2165−2216.
(127) Zhang, J.; Ren, M.; Li, Y.; Tour, J. M. In situ synthesis of efficient water oxidation catalysts in laser-induced graphene. *ACS Energy Lett.* **2018**, *3* (3), 677−683.
(128) Wei, Q.; Qi, H.; Luo, W.; Tseng, D.; Ki, S. J.; Wan, Z.; Göröcs, Z. n.; Bentolila, L. A.; Wu, T.-T.; Sun, R.; et al. Fluorescent

https://doi.org/10.1021/acsomega.2c01033
ACS Omega 2022, 7, 22073−22088

imaging of single nanoparticles and viruses on a smart phone. *ACS Nano* **2013**, *7* (10), 9147−9155.
(129) Zhu, H.; Fohlerová, Z.; Pekárek, J.; Basova, E.; Neužil, P. Recent advances in lab-on-a-chip technologies for viral diagnosis. *Biosens. Bioelectron.* **2020**, *153*, 112041.
(130) Parihar, A.; Ranjan, P.; Sanghi, S. K.; Srivastava, A. K.; Khan, R. Point-of-care biosensor-based diagnosis of COVID-19 holds promise to combat current and future pandemics. *ACS Appl. Bio Mater.* **2020**, *3* (11), 7326−7343.
(131) Zhao, L.; Wu, Z.; Liu, G.; Lu, H.; Gao, Y.; Liu, F.; Wang, C.; Cui, J.; Lu, G. High-activity Mo, S co-doped carbon quantum dot nanozyme-based cascade colorimetric biosensor for sensitive detection of cholesterol. *J. Mater. Chem. B* **2019**, *7* (44), 7042−7051.
(132) Shi, W.; Li, J.; Wu, J.; Wei, Q.; Chen, C.; Bao, N.; Yu, C.; Gu, H. An electrochemical biosensor based on multi-wall carbon nanotube-modified screen-printed electrode immobilized by uricase for the detection of salivary uric acid. *Anal. Bioanal. Chem.* **2020**, *412* (26), 7275−7283.
(133) Narita, F.; Wang, Z.; Kurita, H.; Li, Z.; Shi, Y.; Jia, Y.; Soutis, C. J. A. M. A review of piezoelectric and magnetostrictive biosensor materials for detection of COVID-19 and other viruses. *Adv. Mater.* **2021**, *33* (1), 2005448.
(134) Mao, S.; Chang, J.; Zhou, G.; Chen, J. J. S. Nanomaterial-enabled Rapid Detection of Water Contaminants. *Small* **2015**, *11* (40), 5336−5359.

https://doi.org/10.1021/acsomega.2c01033
ACS Omega 2022, 7, 22073−22088